ELSEVIER

Thermochimica Acta 293 (1997) 47–63

thermochimica acta

A new analyzing method of temperature modulated DSC of exo- or endo-thermic process: Application to polyethylene crystallization

Akihiko Toda[a,*], Tatsuro Oda[a], Masamichi Hikosaka[a], Yasuo Saruyama[b]

[a] *Faculty of Integrated Arts and Sciences, Hiroshima University, 1-7-1 Kagamiyama, Higashi-Hiroshima 739, Japan*
[b] *Faculty of Textile Science, Kyoto Institute of Technology, Matsugasaki, Sakyo-ku, Kyoto 606, JAPAN*

Received 19 July 1996; accepted 12 December 1996

Abstract

A new method is presented to analyse an exothermic or endothermic process with temperature modulated differential scanning calorimetry. The response of exo- or endo-thermic process against temperature modulation has been directly taken into account in an apparent heat capacity difference of complex quantity. Utilizing the shift in phase lag between sample temperature and heat flow, the specific heat during the transformation process and the temperature coefficient of the transformation rate, e.g. crystal growth rate, are obtainable by the analysis under a reasonable assumption.The applicability of the present method has been examined with the experimental results of polyethylene crystallization. © 1997 Elsevier Science B.V.

Keywords: DSC; Temperature Modulated; Transformation kinetics; Polyethylene; Crystallization

1. Introduction

Temperature Modulated differential scanning calorimetry (TMDSC) applies a sinusoidal temperature modulation to a conventional DSC run and analyses the response in heat flow [1–3]. The technique is well established in heat capacity determination without exothermic or endothermic process [4–7], and most of the TMDSC studies has been mainly concerned with the change in specific heat during the process such as glass transition. When exothermic and endothermic processes such as crystallization and melting are concerned the development of physical interpretation is essential to analyse the data upon the processes . In a short communication [8], we have recently reported a general treatment of quantitative analysis of the kinetics of exothermic or endothermic process, utilizing the change in phase lag between oscillation components of sample temperature and heat flow. In the present paper, we discuss the details of the method. In the following, we firstly introduce the model and the method to analyse the kinetics. The method is then applied to the isothermal crystallization of polyethylene.

2. Model

2.1. A fundamental equation

Firstly, we introduce a fundamental equation of a classical DTA [9]

*Corresponding author. Tel: +81-(0)824-24-6558; fax: +81-(0)824-24-0757; E-mail: atoda@ipc.hiroshima-u.ac.jp.

PII S0040-6031(97)00051-8

$$C_r\frac{d(\Delta T)}{dt}+\Delta C\frac{dT_s}{dt}=-K\Delta T-\frac{d(\Delta H)}{dt} \quad (1)$$

$$\Delta C\equiv C_s-C_r\cong mc$$

$$\Delta T\equiv T_s-T_r$$

where C_s and C_r represent sample and reference heat capacities, T_s and T_r sample and reference temperatures, K the Newton's law constant, ΔH the enthalpy of the sample, m sample weight, and c specific heat of the sample, respectively. Following the treatment of Wunderlich et at. [4,5], we apply the above equation to TMDSC of heat flux type. Considering the fundamental equation of DSC of heat flux type (e.g. Mraw's model [10]) with the heat capacities of monitoring stations of sample and reference temperatures and the thermal resistance between the sample (reference) and the monitoring station, we have the results in Appendix A, which is essentially similar to the following results.

The sample temperature T_s and the temperature difference ΔT are modulated in the following manner,

$$T_s=\bar{T}_s+\tilde{T}_s e^{i(\omega t+\epsilon)} \quad (2)$$

$$\Delta T=\overline{\Delta T}+\Delta\tilde{T}e^{i(\omega t+\delta)} \quad (3)$$

Here, we consider the process under quasi-isothermal condition ($\overline{T_s}$ constant). The method will be also applicable to the case of heating and cooling with a constant rate, if the rate is slow enough.

2.2. Basic assumption concerning the exo- or endothermic process

The present analysis approximates the development of heat flow due to exo- or endo-thermic process after $t=t_0+\Delta t$ applying the temperature modulation of Eq. (2), as follows,

$$F(t,T_s)\equiv-\frac{d(\Delta H)}{dt}\cong F(t_0,\overline{T_s})+\left(\frac{\partial F}{\partial t}\right)_{t_0,\overline{T_s}}\Delta t+\left(\frac{\partial F}{\partial T}\right)_{t_0,\overline{T_s}}\tilde{T}_s e^{i(\omega t+\epsilon)} \quad (4)$$

The applicability of the expansion about temperature has been implicitly postulated in the original works of Reading [1–3], as is mentioned and outlined in [7]. However, the significance of the consequences discussed below was not seriously considered in those works.

The coefficient, $\left(\frac{\partial F}{\partial T}\right)_{t_0,\overline{T_s}}$, of the expansion of the temperature modulation $\tilde{T}_s e^{i(\omega t+\epsilon)}$ of course experiences a change due to the progress of transformation. Therefore, it is necessary for the following discussion to assume that the change in $\left(\frac{\partial F}{\partial T}\right)$ is small enough during the time interval of the modulation period. On the other hand, the linear response theory [11] claims that this expansion implicitly assumes the instantaneous response of exo- or endo-thermic process without retardation (Appendix B). In general, the response of exo- or endothermic process against a sudden change in temperature needs some retardation time. If we take the retardation time into account, the response of $\left(\frac{\partial F}{\partial T}\right)$ against oscillating temperature becomes a complex quantity: see Appendix B.

2.3. Basic equation of TMDSC

Inserting Eqs. (2)–(4) into Eq. (1), we obtain the following equation satisfied by the oscillating terms,

$$(K+i\omega C_r)\Delta\tilde{T}e^{i(\omega t+\delta)}=-i\omega\left(\Delta C+i\frac{F'_T}{\omega}\right)\tilde{T}_s e^{i(\omega t+\epsilon)} \quad (5)$$

where F'_T is defined as,

$$F'_T\equiv\left(\frac{\partial F}{\partial T}\right)_{t_0,\overline{T_s}} \quad (6)$$

We introduce an apparent heat capacity difference $\Delta\tilde{C}e^{-i\alpha}$, as defined below,

$$\Delta\tilde{C}e^{-i\alpha}\equiv\Delta C+i\frac{F'_T}{\omega} \quad (7)$$

The true heat capacity difference ΔC is a coefficient of heat flow response against $\frac{dT}{dt}$, while F'_T is the coefficient against T. For the sinusoidal modulation, $\frac{dT}{dt}$ and T are at right angles to each other, and hence F'_T is multiplied by $\frac{i}{\omega}$ when translated to the value as a heat capacity. In general, values of both ΔC and F'_T are complex quantities exhibiting relaxation processes (Appendix B and Appendix C). It means that the two types of relaxation processes coexist in the present system.

For the convenience of calculation, we define ΔC_0 as,

$$\Delta C_0 \equiv \frac{K\Delta\tilde{T}}{\omega\tilde{T}_s} \tag{8}$$

where $K\Delta\tilde{T}$ is proportional to the amplitude of modulated heat flow. The value of ΔC_0 can be directly determined from the TMDSC run, and was originally supposed to express the true heat capacity difference [1]. Utilizing the expressions of Eq. (7) and Eq. (8), the magnitude and phase of Eq. (5) can be reorganized as follows,

$$\frac{1}{\Delta C_0}e^{i(\epsilon-\delta)} = \frac{i}{\Delta\tilde{C}}\left(1 + i\frac{C_r}{K}\omega\right)e^{i\alpha} \tag{9}$$

$$\frac{1}{\Delta C_0} = \frac{1}{\Delta\tilde{C}}[1 + \left(\frac{C_r}{K}\omega\right)^2]^{1/2} \tag{10}$$

$$(\epsilon - \delta) = \frac{\pi}{2} + \tan^{-1}\left(\frac{C_r}{K}\omega\right) + \alpha \tag{11}$$

By examining the ω dependence of ΔC_0 in Eq. (10), we are able to determine the quantities $\Delta\tilde{C}$ and (C_r/K) appearing in the right hand side of the equation.

2.4. The case of $F_T'=0$

When $F_T' = 0$ in Eq. (5), the analysis of Wunderlich et al. [4,5] applies to the process; the phase α becomes zero in Eq. (7) and the magnitude of the apparent heat capacity difference $\Delta\tilde{C}$ equals the true heat capacity difference ΔC,

$$\frac{1}{\Delta C_0} = \frac{1}{\Delta C}\left[1 + \left(\frac{C_r}{K}\omega\right)^2\right]^{1/2} \tag{12}$$

$$(\epsilon - \delta)_0 = \frac{\pi}{2} + \tan^{-1}\left(\frac{C_r}{K}\omega\right) \tag{13}$$

The condition of $F_T' = 0$ is satisfied, if the dependence of exo- or endo-thermic process on temperature is negligible, including the case of F=0.

2.5. The case of $F_T' \neq 0$

For the transformation rate dependent on temperature ($F_T' \neq 0$), the phase α in Eq. (11) can be determined by subtracting $(\epsilon-\delta)_0$ of Eq. (13) as a baseline from $(\epsilon-\delta)$ of Eq. (11),

$$\alpha = (\epsilon - \delta) - (\epsilon - \delta)_0 \tag{14}$$

If we are able to assume that ΔC and F_T' are constant and real, we can obtain the true heat capacity difference ΔC and the temperature dependence of the exo- or endo-thermic heat flow, F_T', from $\Delta\tilde{C}$ and α determined from the experimental data of ΔC_0 of Eq. (10) and $(\epsilon-\delta)$ of Eq. (14), as follows,

$$\Delta C = \Delta\tilde{C}\cos\alpha \tag{15}$$

$$F_T' = -\omega\Delta\tilde{C}\sin\alpha \tag{16}$$

This assumption requires that the relaxation and retardation times of the specific heat and the exo- or endo-thermic heat flow are much shorter (or longer) than the modulation period. Compared to the modulation period used in the TMDSC (>ca.30 s), the relaxation time of the specific heat in ΔC will be much shorter under the usual condition, and hence the assumption on ΔC will be justified. The assumption on F_T' is also justified in the case of polymer crystallization, as we will see later.

2.6. Transformation Rate, R

We consider the physical meaning of the exo- or endo-thermic heat flow, F. The change in enthalpy per unit volume Δh and the total transformation rate R gives us the expressions of F and F_T' as

$$F = \Delta hR \tag{17}$$

$$F_T' = \Delta h\frac{dR}{dT} \tag{18}$$

Therefore, the ratio of those quantities gives the temperature dependence of ln R.

$$\frac{d(\ln R)}{dT} = \frac{F_T'}{|F|} \tag{19}$$

2.7. Polymer Crystallization

Polymer crystallization, in general, can be considered as the growth of spherulite or axialite formed by lamellar crystals. In most cases, high supercooling (>ca.10°C) is necessary for polymer crystallization, and hence the response of the kinetics against the

small temperature modulation (~ ca. ±0.2°C) is supposed to be a periodic change in growth rate, while reversible crystallization and melting should be the case at the melting temperature. Therefore, the total transformation rate R can be expressed by the crystal growth rate G multiplied by the total area of growth face S_{total} as $R = GS_{\text{total}}$. Then, Eq. (17), Eq. (18) and Eq. (19) are expressed by the growth rate, as follows,

$$F = \Delta h S_{\text{total}} G \tag{20}$$

$$F'_{\text{T}} = \Delta h S_{\text{total}} \frac{\mathrm{d}G}{\mathrm{d}T} \tag{21}$$

$$\frac{\mathrm{d}(\ln G)}{\mathrm{d}T} = \frac{F'_T}{F} \tag{22}$$

When ΔC and F'_T are constant and real, we obtain the following relationship from Eq. (16) and Eq. (22),

$$\frac{\mathrm{d}(\ln G)}{\mathrm{d}T} = -\frac{\omega \Delta \tilde{C} \sin\alpha}{F} \tag{23}$$

Eq. (23) suggests that the temperature dependence of crystal growth rate can experimentally be determined by the quantities in the right hand side of the equation, where the exothermic heat flow F can be evaluated from the total heat flow of TMDSC.

3. Experimental

The DSC 2920 Module controlled with Thermal Analyst 2200 (TA Instruments) was used for all measurements.The raw data were transferred by a TA RMX Utility to calculate the phase lag $(\epsilon-\delta)$ from the raw data of modulated sample temperature and of modulated heat flow. The value of ΔC_0 was obtained by setting the calibration constant of heat capacity as unity. The sample was a fractionated polyethylene (PE-A: NIST SRM1483, M_w=3.21×10^4 and M_w/M_n =1.11) or an unfractionated one (PE-B: NIST SRM1475, M_w=5.2×10^4 and M_w/M_n =2.9). The samples with weight of 1–7 mg were examined. It was confirmed that there was no qualitative change by the sample weight in this range. The mode of TMDSC run was basically quasi-isothermal, modulation around a constant temperature. The modulation period of 20–100 s was examined with the modulation amplitude fixed at ±0.2 K.

4. Results and Discussion

4.1. The case of F_T'=0

We need to confirm the applicability of the Wunderlich's analysis [4,5] Eq. (12) and Eq. (13) to the case of $F'_T = 0$ by examining the behaviour at temperatures where no crystallization or melting occurs. We have done the TMDSC measurements at 50 and 160°C which is above the melting point, and at 133°C without introducing crystallization after melting at 160°C; above 131°C under usual condition, no detectable crystallization of polyethylene occurs. There were no qualitative difference among those results, and hence we show the results only at 133°C in the following.

Firstly,Fig. 1a shows the plots of $\left(\frac{1}{\Delta C_0}\right)^2$ against the angular frequency squared ω^2. The data points for the periods of modulation larger than 24 s are well fitted to a straight line and confirms the relationship of Eq. (12). From the slope and the intercept, we obtain $\frac{C_r}{K}$ and the true heat capacity difference $\Delta C(=\Delta\tilde{C})$. The deviation of the values of $\Delta C \cong mc$ at each temperature was within several percent from the values reported by Gaur and Wunderlich [13]. Concerning the systematic deviation from the linear relationship at higher frequencies in Fig. 1, it is mainly due to the failure of temperature control at such high frequencies of modulation, which is apparently seen in the Lissajous diagram of Fig. 2.

Secondly, Fig. 1 b shows the ω dependence of the phase lag $(\epsilon-\delta)_0$. In Fig. 1 b, $\tan^{-1}\left(\frac{C_r}{K}\omega\right)$ is also plotted, using the value of $\frac{C_r}{K}$ determined from the linear fitting in Fig. 1 a. Fig. 1 b also shows the resultant excess of phase delay $\phi_0 \equiv (\epsilon-\delta)_0 - \tan^{-1}\left(\frac{C_r}{K}\omega\right)\frac{\pi}{2}$ which should vanish if Eq. (13) is exact. The excess phase delay can be fitted to a straight line for smaller ω, and hence the phase delay may be approximated as $\tan^{-1}(\omega\tau_0)$, where the time τ_0 is about 2–3 s. Appendix A shows that the excess phase delay of this type is expected from more general equations of DSC of heat flux type. Such a phase delay can also be incorporated by assuming a complex

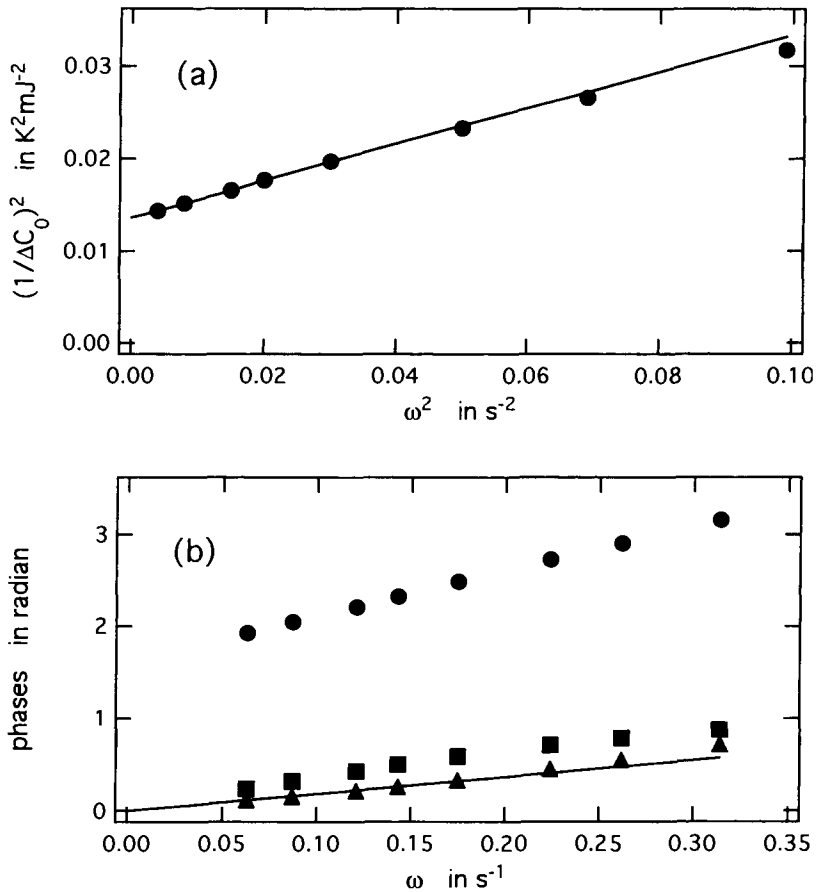

Fig. 1. Plots of (a) $(\frac{1}{\Delta C_0})^2$ against ω^2 and (b) $(\varepsilon - \delta)_0$ (●), $\tan^{-1}(\frac{C_r}{K}\omega)$ (■) and ϕ_0 (▲) against ω. The modulation periods were 20, 24, 28, 36, 44, 52, 72 and 100 s. Temperature was quasi-isothermal at 133.0°C after melting at 160.0°C. The sample was PE-A of 3.28 mg

value of the Newton's law constant K [12]. The actual phase lag $(\epsilon-\delta)_0$ is then expressed as follows, instead of Eq. (13),

$$(\epsilon - \delta)_0 = \frac{\pi}{2} + \tan^{-1}\left(\frac{C_r}{K}\omega\right) + \phi_0 \qquad (24)$$

where $\phi_0 = \tan^{-1}(\omega\tau_0)$.

From the above discussions, we can conclude that Eq. (12) and Eq. (24), which were originally derived by Wunderlich et al. [4,5], well explain the TMDSC data in the case of $F_T' = 0$, if we introduce the instrumental phase delay ϕ_0 in Eq. (24). In the following discussion, we use the value of $\frac{C_r}{K}$ obtained at 133°C in order to convert the data of ΔC_0 during the isothermal crystallization at 125–130°C to $\Delta\tilde{C}$ by Eq. (10).

4.2. *A typical raw data of isothermal crystallization of PE: $F_T' \neq 0$.*

Fig. 3 shows a typical TMDSC data of F, $\Delta\tilde{C}$, and $(\epsilon-\delta)$ during isothermal crystallization. Following the crystallization the rate of which shows a maximum in the exothermic heat flow F, we can confirm the increase in $\Delta\tilde{C}$ up to a maximum followed by a gradual decrease. We will discuss below whether it is due to the change in the true heat capacity ΔC or not. From Fig. 3, it is also clearly seen that the progress of the change in phase lag $(\epsilon-\delta)$ is quite similar to that of exothermic heat flow F; we will also discuss the point below. It should be noted that the oscillating magnitude of 2ω component in the raw data of modulated heat flow was negligibly smaller (< ca.

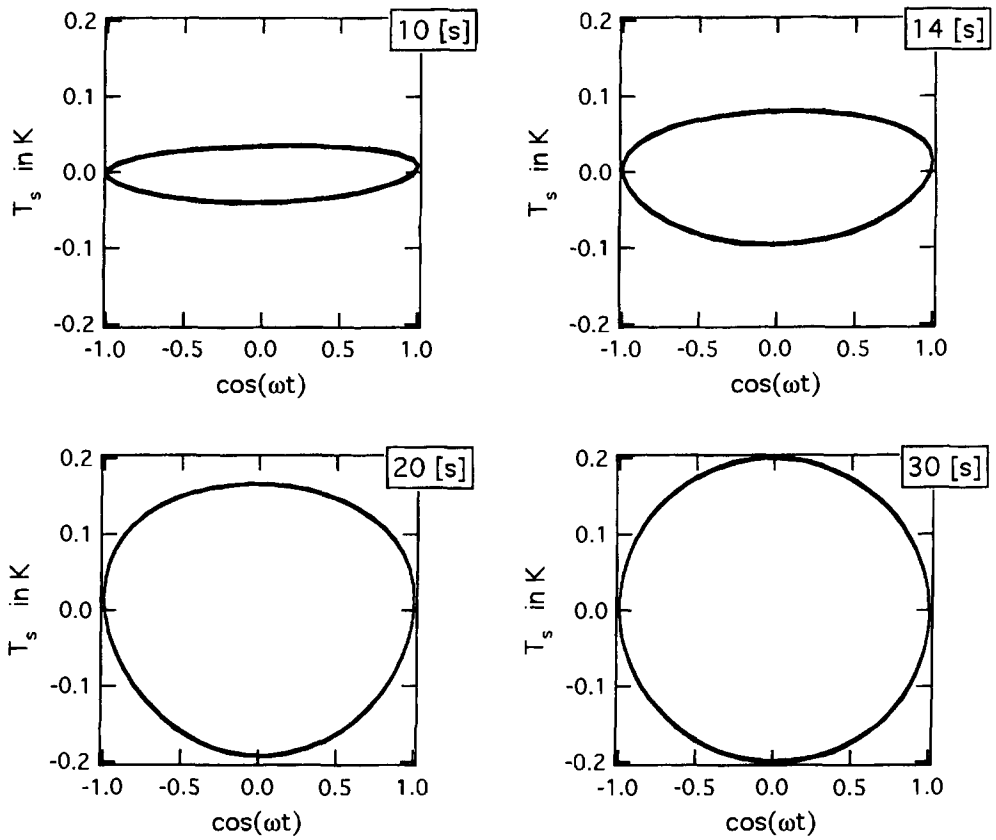

Fig. 2. Lissajous diagrams of T_s against cos ωt. The periods of temperature modulation are indicated. Temperature was quasi-isothermal at 50.0°C. The sample was PE-B of 4.01 mg.

1%) than that of ω component, and hence we can justify the present analysis within the framework of linear response, at least in the case of polyethylene crystallization.

4.3. ω dependence of $\Delta\tilde{C}e^{-i\alpha}$

We examine the frequency dependence of $\Delta\tilde{C}e^{-i\alpha}$ during crystallization, in order to confirm that ΔC and F'_T in Eq. (7) can be approximately considered constant and real for polyethylene crystallization with the modulation period used in the standard TMDSC (> ca. 20 s). We crystallized the sample by cooling at a very slow rate of 0.01°K min^{-1} in the temperature range 130–126°C at several modulation periods of 24–100 s (Fig. 4); we assume that the present method is applicable to such a slow cooling rate of TMDSC run. From the change in the exothermic heat flow in Fig. 4a, we can confirm that the progress of crystallization is not affected by the change of modulation period. Fig. 5 shows the real and imaginary parts of $\Delta\tilde{C}e^{-i\alpha}$ calculated from ΔC_0 and α shown in Fig. 4 b and c. It is clearly seen that the imaginary part is quite smaller than the real part, while the ω dependence of the imaginary part is large.

In order to examine the frequency dependence, we plotted the data of the real and imaginary parts at 128.0, 127.5 and 127.0°C against ω and $\frac{1}{\omega}$ in Fig. 6 a and b, respectively; we consider the data at each temperature represent the same degree of crystallization irrespective of the modulation periods. Fig. 6a shows that the real part stays almost constant, while the imaginary part in Fig. 6b is proportional to $\frac{1}{\omega}$. Therefore, we can practically consider that ΔC and F'_T in Eq. (7) are constant and real and hence the real and imaginary parts of $\Delta\tilde{C}e^{-i\alpha}$ represent ΔC and $\frac{F'_T}{\omega}$,

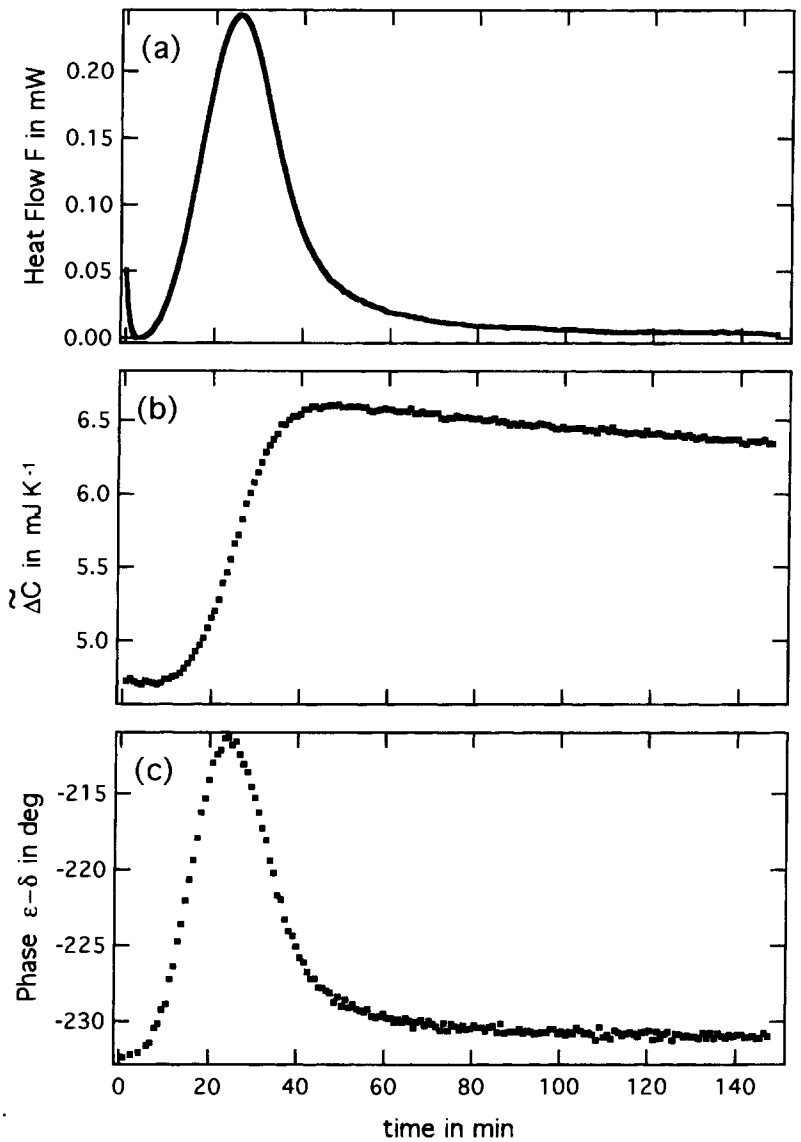

Fig. 3. A typical TMDSC results of polyethylene crystallization: (a) the exothermic heat flow F, (b) $\Delta\tilde{C}$ and (c) phase lag ($\epsilon-\delta$). Temperature was quasi-isothermal at 127.5°C. The sample was PE-A of 1.71 mg.

respectively, (Eq. (15) and Eq. (16)), for polyethylene crystallization with the modulation periods of 20–100 s.

4.4. *The correction of* $\Delta C = \Delta\tilde{C}\cos\alpha$

The requirement of the correction of $\Delta C = \Delta\tilde{C}\cos\alpha$ in Eq. (15) is well demonstrated in Fig.(7) where we plotted the sequences of $\Delta\tilde{C}$ and ΔC for different modulation periods during isothermal crystallization.The crystallization is relatively fast at the temperature and hence the contribution of F'_T becomes large. Under the condition, the curve of $\Delta\tilde{C}$ in Fig. 7 a exhibits an apparent peak following the peaks in F and ($\epsilon-\delta$). The peak is only apparent when ω is sufficiently small, in other words when the imaginary part $\frac{F'_I}{\omega}$ of

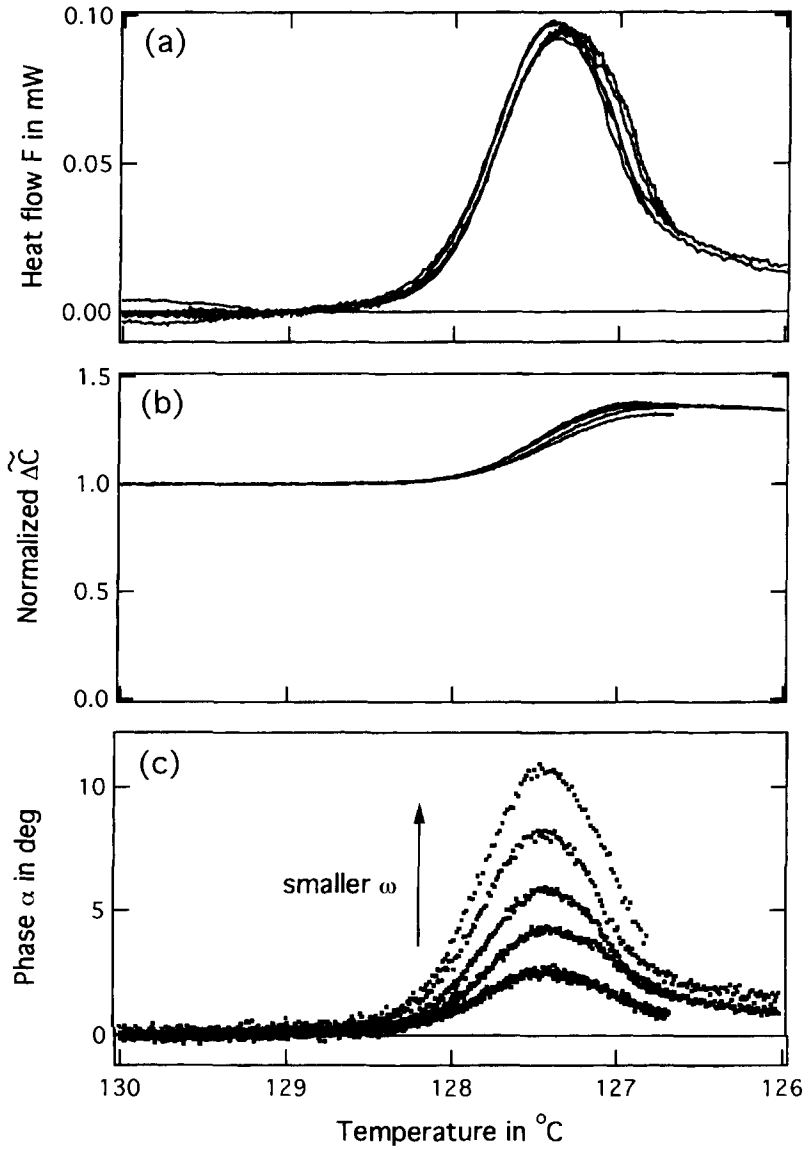

Fig. 4. TMDSC results of polyethylene crystallization: (a) the exothermic heat flow F, (b) $\Delta\tilde{C}$ and (c) α, taking the value of $(\epsilon-\delta)_0$ at 129.5°C. $\Delta\tilde{C}$ is normalized by the value at 129.5°C. The modulation periods were 24, 36, 52, 72 and 100 s. Temperature was cooled down at 0.01°K/min from 130.0 to 126°C after melting at 160°C. The sample was PE-B of 3.06 mg.

Eq. (7) is sufficiently large. The plots of ΔC shown in Fig. 7b, on the other hand, are on a single master curve without the peaks.

The true heat capacity difference $\Delta C \cong mc$ in Fig. 7b shows an increase up to a maximum and then a gradual decrease, following the progress of crystallization as stated in Section 4.2. The overall heat capacity of the sample is expected to change due to the increase in the degree of crystallinity. By the Avrami plot of both ΔC and the degree of crystallinity determined from the integration of F, we can confirm that the increase in ΔC up to the maximum corresponds to the change in the degree of crystallinity (Fig. 8); both the plots give the same Avrami constant

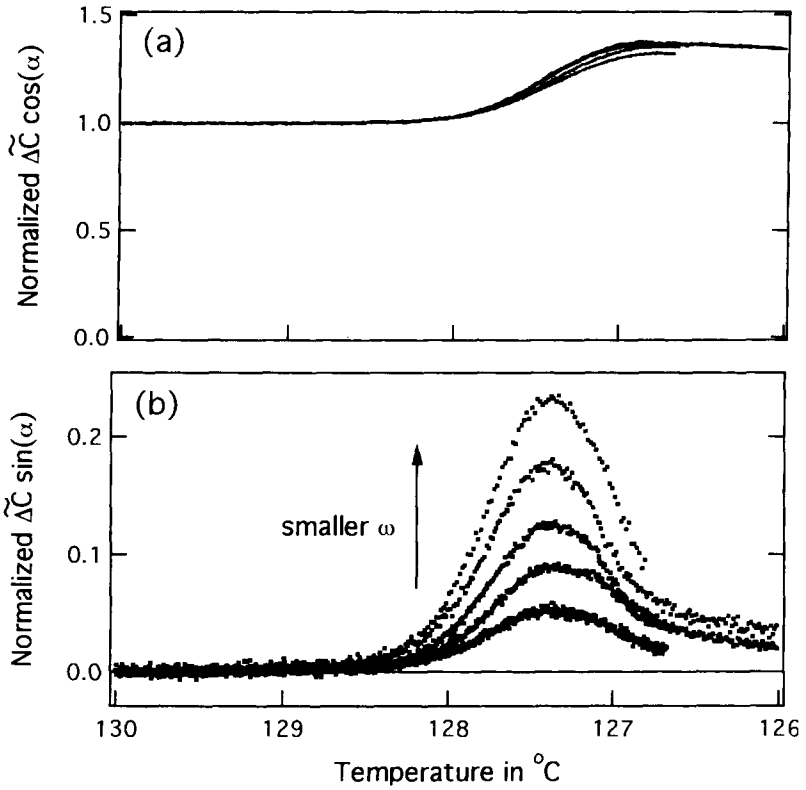

Fig. 5. Plots of the (a) real and (b) imaginary parts of $\Delta\tilde{C}e^{-i\alpha}$ calculated from $\Delta\tilde{C}$ and α shown in Fig 4b and c.

3.4. This conclusion means that the specific heat of crystals is larger than that of the melt at the crystallization temperatures which are not far from the melting point. Such an inverted relationship near the melting point has already been reported by Gaur and Wunderlich [13]. By the present experiments, it is found that the specific heat of crystals gradually decreases by the passage of time. The decrease in ΔC continues after the completion of crystallization, and hence it will be due to an annealing effect in the crystals.

4.5. F'_T and $\frac{d(\ln G)}{dT}$

Fig. 9a shows the plots of sin α overlapped with the exothermic heat flow F for a typical TMDSC data of isothermal crystallization. It is clearly seen that sin α traces the progress of F except for the later stage. If we plot $\frac{d(\ln G)}{dT}$ determined from Eq. (23), the result of (i) in Fig. 9 b shows that $\frac{d(\ln G)}{dT}$ keeps a constant value in the vicinity of the peak of exothermic heat flow, namely during the linear growth of spherulites or axialites.

We notice the systematic deviation of $\frac{d(\ln G)}{dT}$ of (i) in Fig. 9 b from its mean value in the later stage of growth, which must be due to the shift in the baseline of sin α in Fig. 9 a. The shift is quite small (a few degrees) but definite. Such a trend can also be seen in Fig. 4 c. As discussed in Appendix C, the shift will be due to the imaginary part of the specific heat, which we have neglected in the above discussion; the effect was not appreciable in the analysis of Section 4.3 because we were concerned with the data in the vicinity of the peak of exothermic heat flow. The existence of the imaginary part of the specific heat with such long modulation periods of 24–100 s must be related to the gradual decrease in the specific heat of crystals shown in Fig. 3 b (or Fig. 7 b); both the behaviours require freedom of very slow motion which may be related to the process of lamellar

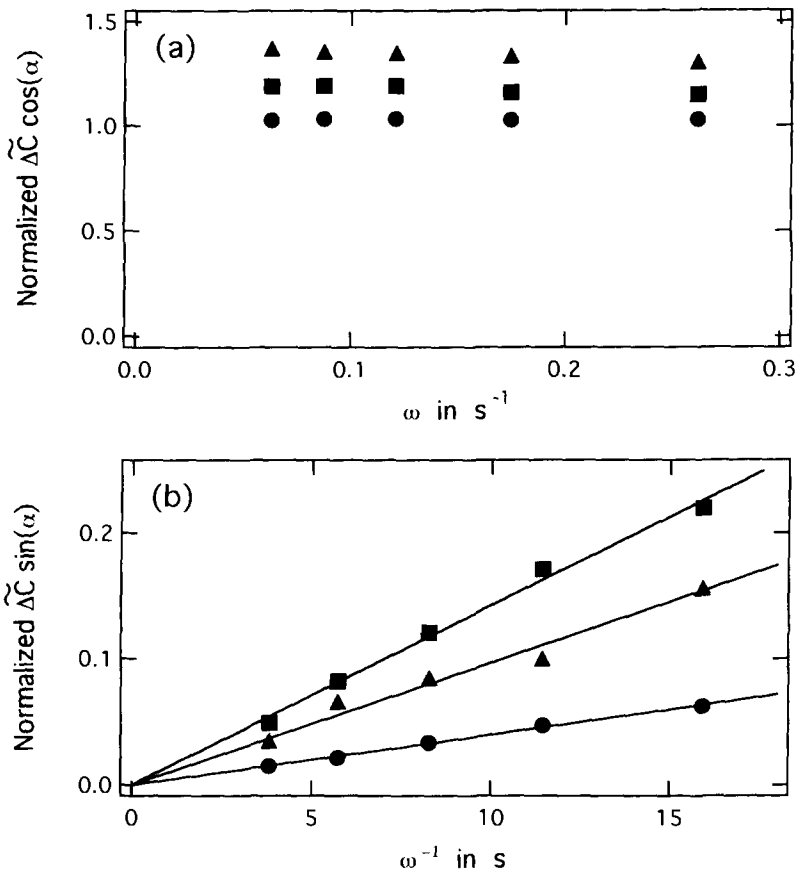

Fig. 6. Plots of (a) the real part of $\Delta\tilde{C}e^{-i\alpha}$ at 128.0 (●), 127.5 (■) and 127.0°C (▲) in Fig. 5a against ω and (b) the imaginary part in Fig 5b against $\frac{1}{\omega}$.

thickening activated near the melting point in the crystals.

Following the method introduced in Appendix C, we set a new baseline which follows the change in the degree of crystallinity determined by the integration of the exothermic heat flow, as shown in Fig. 10 a. The result of the subtraction is shown in Fig. 10 b; sin α' traces the progress of F in the whole range of the data. The plots of the corrected $\frac{d(\ln G)}{dT}$ are shown in Fig. 9 b as (ii), which keeps a constant value in a wider range of crystallization time. The temperature dependence of growth rate, $\frac{d(\ln G)}{dT}$, of (ii) still shows a small deviation from the mean value in the later stage of growth. The deviation means a stronger dependence on temperature and will be due to molecular weight fractionation in the later stage.

At several crystallization temperatures, we have obtained the constant values of the corrected $\frac{d(\ln G)}{dT}$ in the linear growth region. The results are plotted in Fig. 11 b with the results of the direct measurements of linear growth rate by optical microscopy [14]. Both the results agree with each other well and confirm the validity of the present method.

5. Conclusions

We examined the contribution of exo- or endo-thermic process to TMDSC by analyzing the fundamental equation of DSC of heat flux type. The effect of exo- or endo-thermic process has been considered, introducing an apparent heat capacity difference

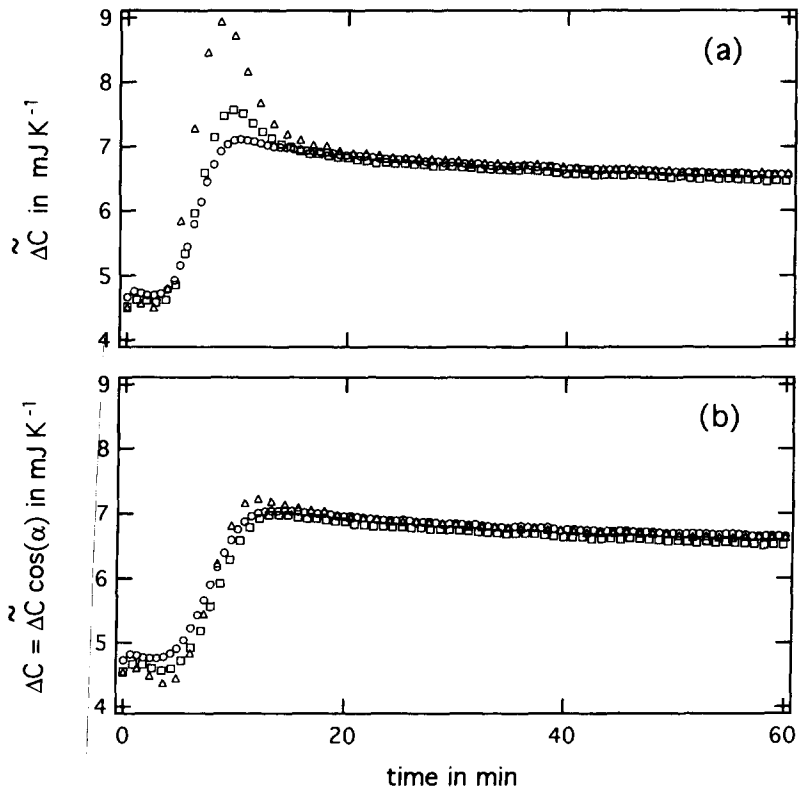

Fig. 7. Time sequence of (a) $\Delta\tilde{C}$ and (b) $\Delta C = \Delta\tilde{C}\cos\alpha$ during quasi-isothermal crystallization at 126.5°C. The periods of temperature modulation are 36 (○), 52 (□), and 72 s (△). The sample was PE-A of 1.71 mg.

$\Delta\tilde{C}e^{-i\alpha}$ which comprises of two different relaxation processes: the specific heat of sample as a coefficient of $\frac{dT}{dt}$ in the response of heat flow and the temperature dependence of exo- or endo-thermic heat flow, F_T', as a coefficient of T. The complex quantity of the apparent heat capacity difference is related to the change in the phase lag between oscillation components of sample temperature and of heat flow by Eq. (11), Eq. (13) and Eq. (14). It has been shown that the specific heat and F_T' can be determined from the experimental data, if the imaginary parts of the specific heat and F_T' are negligibly small.

The present analysis guarantees that we are able to treat the apparent heat capacity difference $\Delta\tilde{C}$ as the true difference ΔC, if the deviation of $(\epsilon-\delta)$ from its baseline $(\epsilon-\delta)_0$ is negligible; the smaller deviation (the smaller α in Eq. (7)) only means the weaker dependence of the transformation rate on temperature (the smaller F_T') and does not necessarily mean the smaller magnitude of exo- or endo-thermic heat flow F itself.

Experimentally, the present model has been successfully applied to polyethylene crystallization. Firstly, we have examined the analysis of Wunderlich et al. [4,5], which is the basis of the present model and is applicable to the case of $F_T' = 0$. We have seen that Eq. (12) and Eq. (24) derived from the analysis well explain the TMDSC data in the temperature range without melting or crystallization, if we introduce the instrumental phase delay ϕ_0 in the phase lag and if the temperature control of the furnace is satisfactory. Secondly, we have applied the present analysis to polyethylene crystallization from the melt. It has been confirmed that the imaginary parts of the specific heat and of F_T' are negligibly small in the case of polyethylene crystallization with the modulation period of 20–100 s; we can assume that ΔC and $\frac{F_T'}{\omega}$ in Eq. (7) represent the real and imaginary parts of $\Delta\tilde{C}e^{-i\alpha}$,

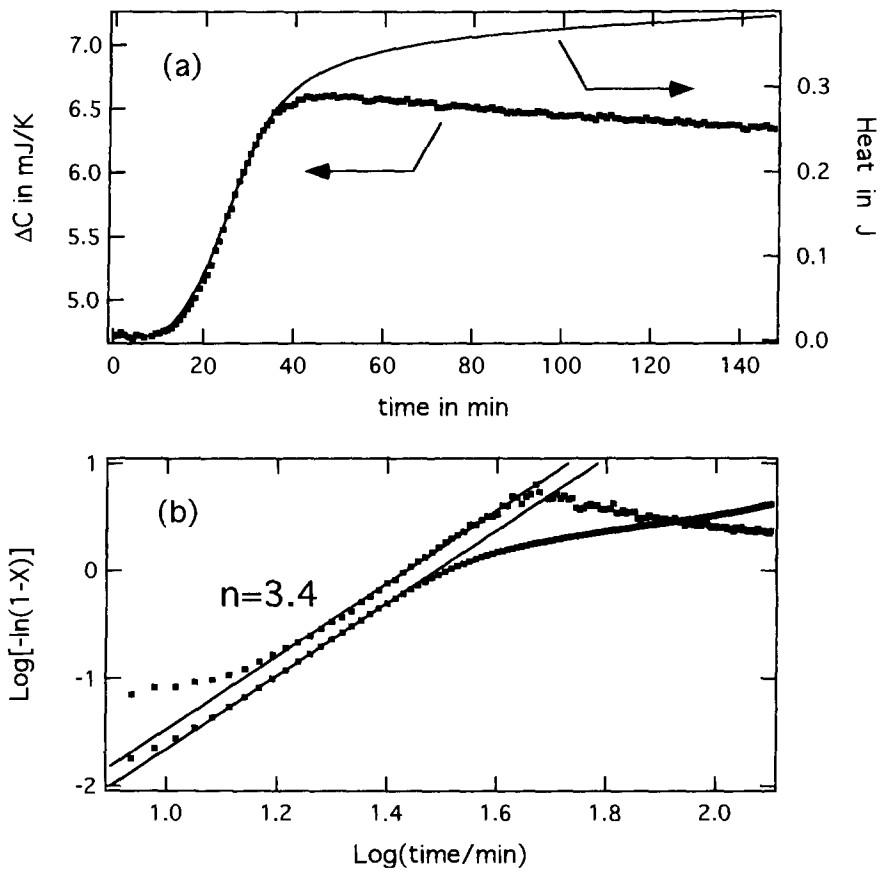

Fig. 8. Plots of (a) the time sequence of ΔC overlapped with the integration of F and (b) their Avrâmi plots during quasi-isothermal crystallization at 127.5°C. The value of X in (b) is either ΔC normalized by the maximum value or the integration of F normalized by the final value. The period of temperature modulation was 52 s. The sample was PE-A of 1.71 mg.

respectively (Eq. (15) and Eq. (16)). The appearance of a peak in $\Delta\tilde{C}$ of Fig. 7 a demonstrated the importance of the correction of Eq. (15). It has also been shown that the temperature dependence of crystal growth rate $\frac{d(\ln G)}{dT}$ can be determined by taking the ratio of F'_T and the exothermic heat flow F (Eq. (23)). The obtained dependence shown in Fig. 11 b well agrees with the values determined from the direct measurements of the linear growth rate by optical microscopy. This method has a great advantage compared to more indirect method e.g. plotting the half time of crystallization, $\tau_{0.5}$, against temperature.

The present method will be applicable not only to polymer crystallization but also to a wider range of exo- and endo-thermic processes, e.g. polymer melting, chemical reaction including epoxy cure, polymer gelation, etc. It has been reported that the melting of poly(ethylene terephthalate) crystals shows quite large peaks in the magnitude of the apparent heat capacity difference $\Delta\tilde{C}$ and in the phase lag $(\epsilon-\delta)$ [3]. The melting of polyethylene is also followed by a large peak in $\Delta\tilde{C}$ [15]. Those peaks will be relevant to the strong dependence of melting rate on temperature and to the relaxation process of melting, the retardation time of which is comparable to the modulation period; the details of the crystallization and melting of poly(ethylene terephthalate) will be the subject of a forthcoming paper.

Finally, it is noted that the temperature modulation using conventional DSC has a lower limit of the period (ca.20–30 s for the amplitude of ±0.2°C) below which the temperature control of the furnace fails. In order to

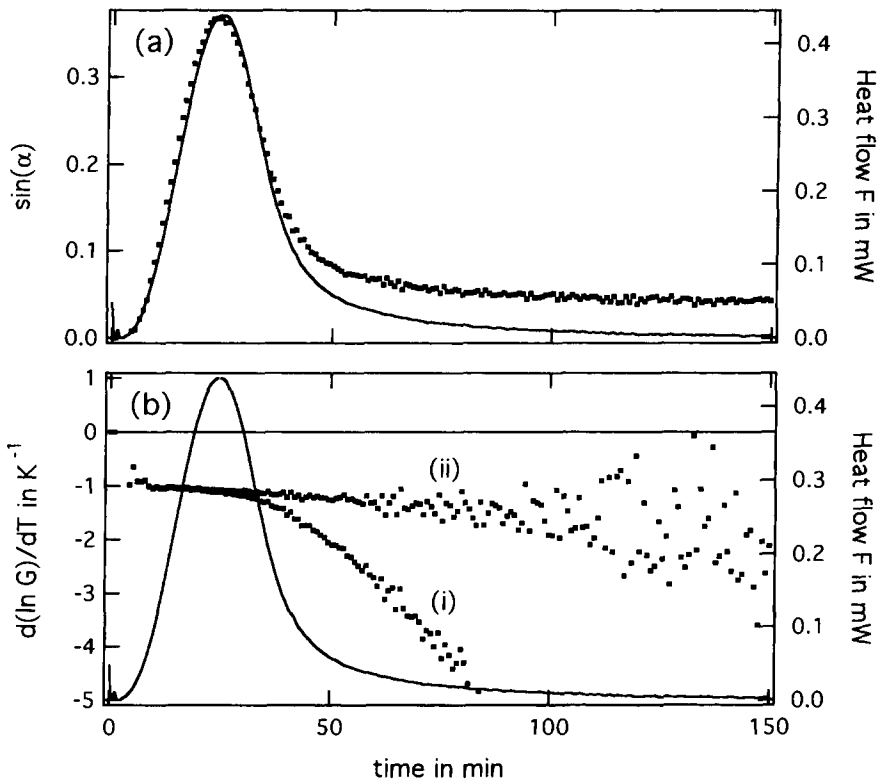

Fig. 9. Time sequences of (a) sin(α) and (b) $\frac{d\ln G}{dT}$ overlapped with the exothermic heat flow F during quasi-isothermal crystallization at 127.5°C. Eq. (23) determines $\frac{d\ln G}{dT}$ of (i) and (ii) from the experimental data of sin(α) shown in Fig.9a and sin(α') in Fig. 10b, respectively. The periods of temperature modulation was 52 s. The sample was PE-A of 3.28 mg.

examine the frequency dependence of the relaxation of ΔC and F'_T, the range of frequency is not sufficiently large; this is the reason why we could assume that ΔC and F'_T are constant and real for polyethylene crystallization within the range of modulation period of 20–100 s. In order to examine the retardation time of crystallization or melting, we may need other techniques such as AC calorimetry or a new technique of Light Heating Dynamic DSC [12,16] which can provide a wider range of frequency and especially extend to higher frequencies.

Acknowledgements

This work was partly supported by a Grant-in-Aid for Scientific Research from the Ministry of Education, Science and Culture of Japan and by NEDO International Joint Research Program.

Appendix A

Mraw's model of DSC of heat flux type [10]

Considering the heat capacities of monitoring stations of sample and reference temperatures, C_m, and the thermal resistance between the sample (reference) and the monitoring stations, $1/K'$, we have the following equations of DSC of heat flux type [10]

$$K'(T_{sm} - T_s) = C_s \frac{dT_s}{dt} + \frac{d(\Delta H)}{dt} \quad (A.1)$$

$$K(T_b - T_{sm}) = C_m \frac{dT_{sm}}{dt} + K'(T_{sm} - T_s) \quad (A.2)$$

$$K'(T_{rm} - T_r) = C_r \frac{dT_r}{dt} \quad (A.3)$$

$$K(T_b - T_{rm}) = C_m \frac{dT_{rm}}{dt} + K'(T_{rm} - T_r) \quad (A.4)$$

where T_{sm}, T_{rm} represent the monitored sample and

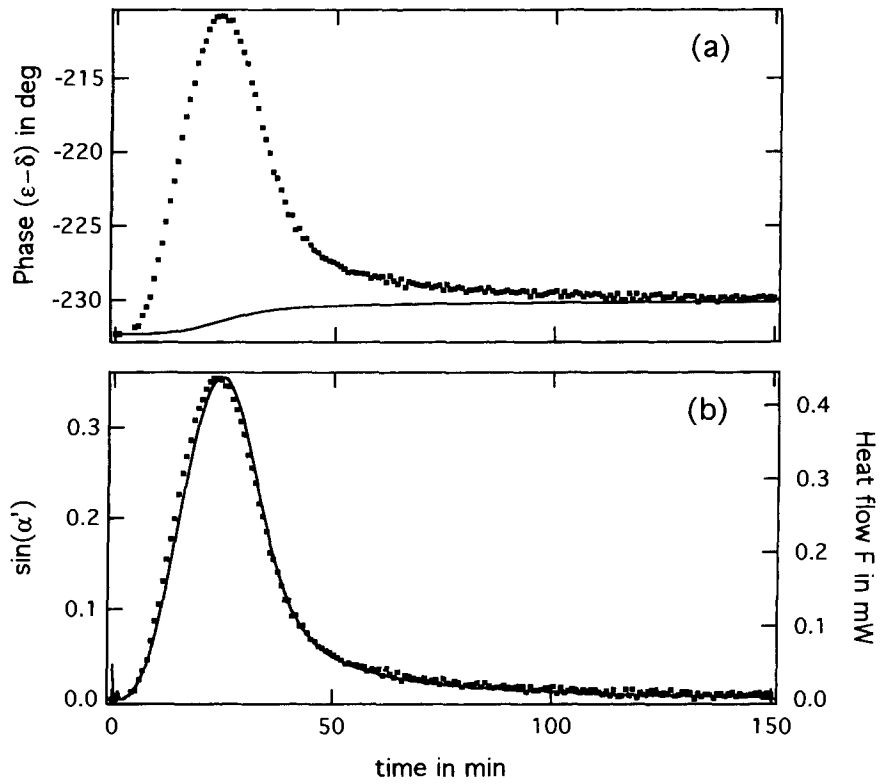

Fig. 10. Time sequences of (a) (ϵ - δ) and (b) sin(α') overlapped with the exothermic heat flow F for the same experimental data as in Fig.9. The new baseline following the change in the degree of crystallinity, $\Delta\gamma$ (t), is plotted in (a).

reference temperatures, respectively, and T_b the block temperature. We have assumed the symmetrical construction of the sample and reference sides. For the sinusoidal modulations of the monitored sample temperature $T_{ms}(=\overline{T_{ms}}+\tilde{T}_{ms}e^{i(\omega t+\epsilon_m)})$ and of the monitored temperature difference $\Delta T_m(=\Delta\overline{T}_m+\Delta\tilde{T}_m e^{i(\omega t+\delta_m)})$, the relationship corresponding to Eq. (5) is expressed as follows,

$$E[K+i\omega(C_r+C_m)]\Delta\tilde{T}_m e^{i(\omega t+\delta_m)} = -i\omega\left(\Delta C+i\frac{F_T'}{\omega}\right)\tilde{T}_{ms}e^{i(\omega t+\epsilon_m)} \quad (A.5)$$

$$E\equiv\left(1-\frac{F_T'}{K'}+i\omega\frac{C_s'}{K}\right)\cdot\left\{1+i\omega\frac{C_r}{K'}\left[\frac{K+i\omega C_m}{K+i\omega(C_r+C_m)}\right]\right\} \quad (A.6)$$

Compared to Eq. (5), it is apparent that the excess phase delay ϕ_0 in Eq. (24) is derived from the factor E in the above equation.

Appendix B

The response of exo- or endo-thermic process as a complex quantity

Following a step wise change in temperature, the exo- or endo-thermic heat flow, in general, responds with retardation, as shown in Fig. 12. If we can apply the principle of superposition to the process, the response of exo- or endo-thermic heat flow $F(t)$ is expressed as,

$$F(t)-F(-\infty)=\int_{-\infty}^{t}S(t-t')\mathrm{d}F=\int_{-\infty}^{t}S(t-t')\frac{dF}{dT}\frac{dT}{dt'}dt' \quad (B.1)$$

where $S(t)$ represents the normalized response function. Against a sinusoidal temperature modulation, the coefficient of the response becomes a complex

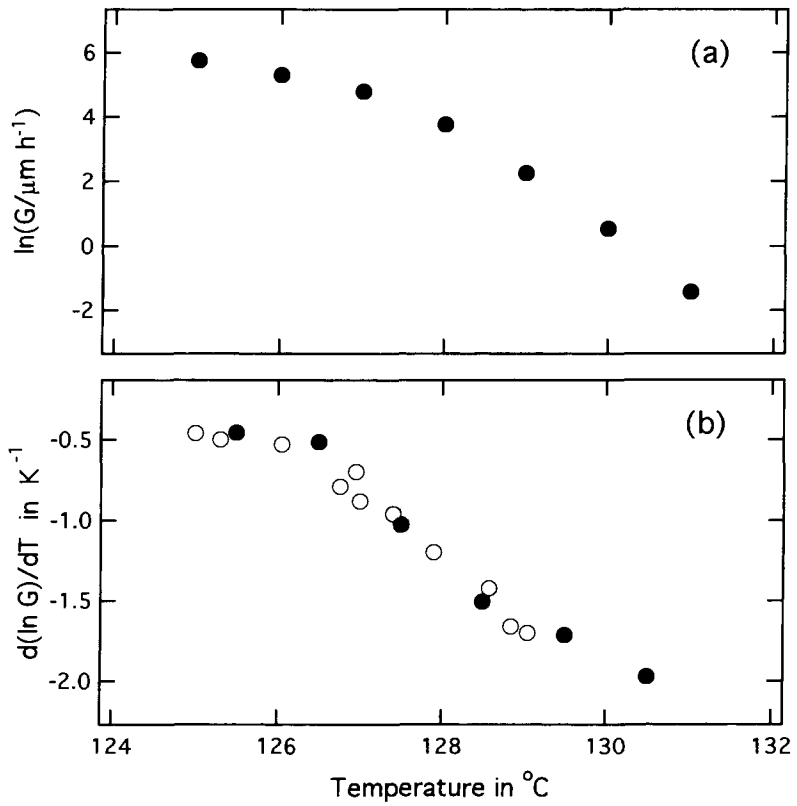

Fig. 11. Plots of (a) linear growth rate, G, of polyethylene spherulites or axialites against temperature and (b) the temperature dependence $\frac{d\ln G}{dT}$. The experimental data (●) are the results of direct measurements by microscopy [14]. The TMDSC results (○) were determined by Eq. (23), utilizing Eq. (C.5). The period of temperature modulation was 24 or 32 s.

quantity, as follows,

$$T = T_0 + \tilde{T}e^{i\omega t} \tag{B.2}$$

$$F(t) - F(-\infty) \equiv \tilde{T}e^{i\omega t}(f_1 - if_2)$$

$$= \tilde{T}e^{i\omega t}\left(\frac{\partial F}{\partial T}\right)_{T_0}\left[S(0) + \int_0^\infty \frac{dS}{dz}e^{-i\omega z}dz\right] \tag{B.3}$$

As the simplest example, we assume the following form of the normalized response function $S(t)$,

$$S(t) = 1 - e^{-t/\tau} \tag{B.4}$$

where τ is the retardation time. Then, the real and imaginary parts of the coefficient $f_1 - if_2$ in Eq. (B.3) becomes,

$$f_1 - if_2 = \left(\frac{\partial F}{\partial T}\right)_{T_0}\left(1 - \frac{i\omega\tau}{1 + i\omega\tau}\right) \tag{B.5}$$

In the case of the instantaneous response of $\tau=0$, the coefficient is given by $\left(\frac{\partial F}{\partial T}\right)_{T_0}$, and we obtain the expansion of Eq. (4).

Appendix C

Complex quantities of ΔC and F'_T

If we express ΔC and F'_T as complex quantities, Eq. (7) becomes,

$$\Delta C = \tilde{mc}e^{-i\gamma} \tag{C.1}$$

$$F'_T = \tilde{F}'_T e^{-i\zeta} \tag{C.2}$$

$$\Delta\tilde{C}e^{-i\alpha} = \tilde{mc}e^{-i\gamma} + i\frac{\tilde{F}'_T}{\omega}e^{-i\zeta} \tag{C.3}$$

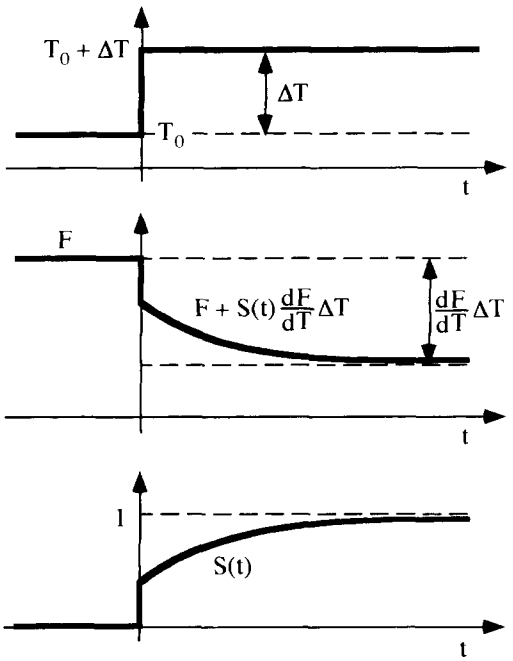

Fig. 12. A schematic time sequence of the response of exothermic heat flow F to a step wise change in temperature T with the normalized response function $S(t)$.

Hence, when $F'_T = 0$, γ is added to $(\epsilon-\delta)_0$,

$$(\epsilon - \delta)_0 = \frac{\pi}{2} + \tan^{-1}\left(\frac{\omega C_r}{K}\right) + \gamma + \phi_0 \qquad \text{(C.4)}$$

The deviation of the phase lag $(\epsilon-\delta)$ from the baseline $(\epsilon-\delta)_0$ is then expressed as,

$$\alpha' \equiv \alpha - \gamma = (\epsilon - \delta) - (\epsilon - \delta)_0 \qquad \text{(C.5)}$$

Therefore, if $\gamma \neq 0$, we obtain the difference $\alpha-\gamma$ instead of α itself from the experimental data of the phase lag. The phase γ undergoes a change during the transformation process such as crystallization because the specific heat of sample changes as,

$$\mathrm{m}\tilde{c}e^{-i\gamma} = \mathrm{m}[x(t)\tilde{c}_s e^{-i\gamma_s} + (1 - x(t))\tilde{c}_l e^{-i\gamma_l}] \qquad \text{(C.6)}$$

where the subscripts of s and l represent the quantities of solid and liquid, respectively, and $x(t)$ the degree of crystallinity. Here, if γ_s and γ_l are small enough, γ in Eq. (C.6) can be approximated by the following,

$$\gamma(t) \cong \gamma_l + x(t)(\gamma_s - \gamma_l)$$
$$= \gamma(0) + \Delta\gamma(t) \qquad \text{(C.7)}$$

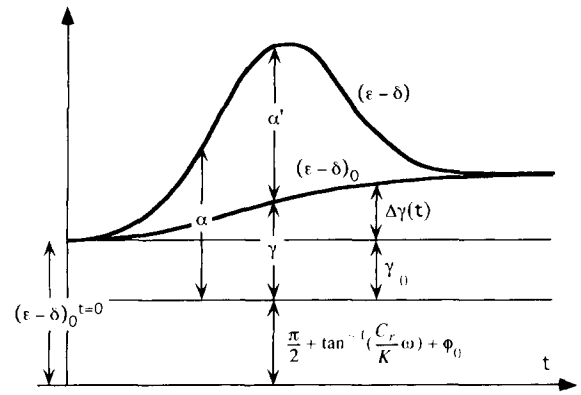

Fig. 13. A schematic time sequence of the phase lag $(\epsilon - \delta)$ during isothermal crystallization.

If we measure the difference of phase lag from the baseline at t=0, we do not obtain the true α' because of the change in γ, as schematically shown in Fig. 13. In order to determine the true α', we must consider the change $\Delta\gamma(t)$ proportional to the degree of crystallinity $x(t)$ which can be evaluated from the integration of the exothermic heat flow.

In general, it is impossible to determine the phases and amplitudes of $\tilde{c}e^{-i\gamma}$ and $\tilde{F}'_T e^{-i\zeta}$ from the experimentally obtainable values of $\Delta\tilde{C}$ and α'. However, if $\zeta - \gamma \ll 1$, we have the following expansion,

$$\Delta\tilde{C}e^{-i\alpha'} = m\tilde{c} + i\frac{\tilde{F}'_T}{\omega}e^{-i(\zeta-\gamma)} \qquad \text{(C.8)}$$

$$\cong m\tilde{c} + \frac{\tilde{F}'_T}{\omega}(\zeta - \gamma) + i\frac{\tilde{F}'_T}{\omega}$$

$$m\tilde{c} = \Delta\tilde{C}\cos\alpha' - \frac{\tilde{F}'_T}{\omega(\zeta - \gamma)} \qquad \text{(C.9)}$$

$$\tilde{F}'_T = -\omega\Delta\tilde{C}\sin\alpha' \qquad \text{(C.10)}$$

Therefore, we have the expression of F'_T similar to Eq. (16). When the specific heat in Eq. (C.9) is concerned the contribution of $\frac{F'_T}{\omega}(\zeta - \gamma)$ may be responsible for the small change in the real part of $\Delta\tilde{C}e^{-i\alpha'}$ shown in Fig. 6a.

References

[1] P.S. Gill, S.R. Sauerbrunn and M. Reading, J. Therm. Anal., 40 (1993) 931.

[2] M. Reading, D. Elliott and V.L. Hill, J. Therm. Anal., 40 (1993) 949.
[3] M. Reading, A. Luget and R. Wilson, Thermochim. Acta, 238 (1994) 295.
[4] B. Wunderlich, Y. Jin and A. Boller, Thermochim. Acta, 238 (1994) 277.
[5] A. Boller, Y. Jin and B. Wunderlich, J. Therm. Anal., 42 (1994) 307.
[6] I. Hatta, Jpn. J. Appl. Phys., 33 (1994) L686.
[7] J.E.K. Schawe, Thermochim. Acta, 260 (1995) 1.
[8] A. Toda, T. Oda, M. Hikosaka and Y. Saruyama, Polymer, 38 (1997) 231.
[9] B. Wunderlich, Thermal Analysis (Academic Press, Boston, MA (1990), chap. 4.
[10] S.C. Mraw, Rev. Sci. Instrum., 53 (1982) 228.
[11] R. Kubo, M. Toda and N. Hashitsume, Statistical Physics II, Springer Series in Solid State Sciences, Springer, Berlin (1991).
[12] Y. Saruyama, Thermochim. Acta, in press.
[13] U. Gaur and B. Wunderlich, J. Phys. Chem. Ref. Data, 10 (1981) 119.
[14] A. Toda, Colloid Polym. Sci., 270 (1992) 667.
[15] Y. Saruyama, J. Thermal Anal., in press.
[16] M. Nishikawa and Y. Saruyama, Thermochim. Acta, 267 (1995) 75.